

Semipolar GaInN/GaN Light-Emitting Diodes Grown on Honeycomb Patterned Substrates

T. Wunderer^{1,*}, J. Wang¹, F. Lipski¹, S. Schwaiger¹, A. Chuvilin², U. Kaiser², S. Metzner³, F. Bertram³, J. Christen³, S. S. Shirokov⁴, A. E. Yunovich⁴, and F. Scholz¹

¹ Institute of Optoelectronics, Ulm University, Ulm, Germany

² Central Facility of Electron Microscopy, Ulm University, Ulm, Germany

³ Institute of Experimental Physics, Otto-von-Guericke-University, Magdeburg, Germany

⁴ Department of Physics, M.V.Lomonosov Moscow State University, Moscow, Russia

Received XXXX, revised XXXX, accepted XXXX

Published online XXXX

PACS 42.72.Bj, 78.55.Cr, 85.60Jb

* Corresponding author: e-mail thomas.wunderer@uni-ulm.de, Phone +49-731-5026454, Fax +49-731-5026049

Excellent semipolar GaN material quality can be obtained by growing inverse GaN pyramids on full 2 inch c-plane sapphire when combining the advantages of defect reduction via FACELO and selective area growth for faceted surfaces. The nearly defect free material is obtained by structuring the mask into a honeycomb pattern. When realizing full GaInN/GaN LED structures on those templates a relatively broad emission is observed during electroluminescence measurements.

Furthermore, the dominant wavelength is found to be dependent on the applied current density. The pronounced shift is in good agreement with the wavelength shift along one single facet. Gas phase diffusion during the active area growth is believed to be the main reason for the varying indium content. The homogeneity could be influenced by changing the reactor pressure during the active area growth.

Copyright line will be provided by the publisher

1 Introduction Non- and semipolar group III-nitrides providing reduced piezoelectric fields are promising candidates for improved device performance due to an increased overlap of the electron and hole wave functions within the quantum wells (QWs) [1]. Nevertheless, one main problem is still limiting the use of non- or semipolar material for commercial production: On foreign substrates with conventional size just inferior material quality compared to c-plane growth can be achieved up to now. In this case, non-radiative recombination is compensating the advantage of the reduced fields and leads to a moderate performance of such devices [2–4]. On the other hand, high quality material can be obtained by cutting pieces from HVPE grown c-plane GaN in the desired direction on which high performance devices were achieved [5]. However, the limited sample size and its high price are still limiting factors for any mass production [6].

In the late 1990s, the technique of facet-controlled epitaxial lateral overgrowth (FACELO) was successfully de-

veloped to reduce the defect density of group III-nitrides [7]. Selective area epitaxy can also be used to form three dimensional (3D) GaN structures with side facets providing semipolar surfaces. Complete semipolar device structures can be obtained on low-cost full 2 inch or larger c-oriented sapphire wafers [8].

In this work, we highlight the possibility to combine the advantages of both techniques, efficient defect reduction via FACELO and the formation of 3D structures providing semipolar GaN surfaces using selective area epitaxy. The 3D structures are used as high quality GaN templates for the implementation of complete LED structures for electroluminescence (EL) test measurements. The unconventional electro-optical properties are analyzed by means of the local layer properties with respect to the structured surface. It is found that the indium composition and QW thickness is varying along a single facet.

Copyright line will be provided by the publisher

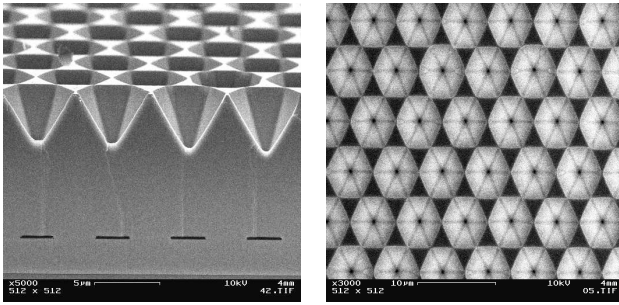


Figure 1 SEM pictures of 3D GaInN/GaN LED structure - bird's eye view (left) and top view (right).

2 Experimental All samples were grown by low pressure metalorganic vapor phase epitaxy (MOVPE). First, about $2\ \mu\text{m}$ thick, high quality GaN was grown on c-plane sapphire wafers including an in-situ deposited SiN interlayer for effective defect reduction [9]. Then, a 200 nm thick SiO_2 layer was deposited via plasma enhanced chemical vapor deposition (PECVD) and structured into a honeycomb pattern serving as a mask for the subsequent selective area growth. Using optimized GaN growth conditions (low temperature, low V/III ratio, high pressure) perfectly ordered inverse pyramids can be realized providing semipolar facets which increase the effectively usable surface. A detailed description on the formation of the 3D structures can be found elsewhere [10]. Realizing a complete LED structure, the 3D GaN template is n-doped, followed by a 5-fold $\text{Ga}_{1-x}\text{In}_x\text{N}/\text{GaN}$ multiple quantum well (MQW) layer stack with a nominal QW thickness of 4 nm and an In concentration x exceeding 30%, a p-AlGaIn electron blocking layer and a p-GaN top layer. For EL test measurements simple indium contacts are realized by standard photo lithography and e-beam evaporation of the metal.

3 Results and discussion Different to previous studies [10] the GaN regrowth in the 2nd epitaxial step was elongated allowing for the coalescence of the material above the masked area. This strategy follows the idea of defect reduction via the FACELO principle. Threading dislocations (TDs) which are not blocked, neither by the in-situ deposited SiN nor the ex-situ deposited SiO_2 mask, and penetrate through the opening are bent to the side due to selective area growth. Using the mask with the honeycomb pattern the TDs are bundled in one point above the mask and (nearly) defect free semipolar facets develop for the subsequent deposition of the active area.

As can be seen in Fig. 1, the 3D surface can be transferred to a higher region above the mask using 3D growth parameters. A planarization of the structure is prohibited whereas it is preferred for typical FACELO samples. Perfectly ordered inverse GaN pyramids are formed providing smooth $\{1\bar{1}01\}$ facets. Transmission electron microscopy (TEM) analyses confirm the efficiency of this technique as no TD could be observed reaching the semipolar surface,

(Fig. 2). They are blocked by the in-situ deposited SiN, the SiO_2 mask or are bent sideways.

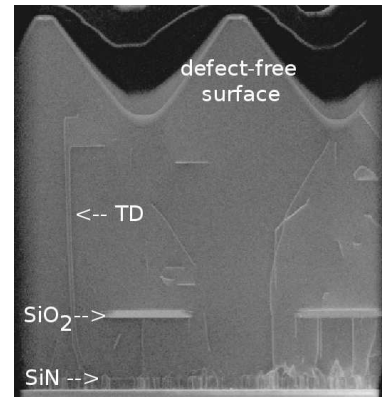


Figure 2 TEM image of inverse pyramid structure showing the efficient defect reduction.

The high material quality is further confirmed via x-ray rocking curve measurements (XRC) and optical investigations using photo- and cathodoluminescence measurements (PL, CL), respectively. The following values displaying the full-width at half maximum (FWHM) of symmetric and asymmetric reflections, respectively, could be obtained from XRC measurements: 299 arcsec for the (00.2), 410 arcsec for the (10.1), 416 arcsec for the (10.2) and 284 arcsec for the (11.2) reflection. Fig. 3 shows the PL spectrum of the 3D GaN recorded at 14 K. No stacking fault-related transition could be observed for the sample as it is typically found for non-polar GaN grown on foreign substrates [13]. The FWHM of the donor-bound exciton transition (D^0X) at 3.479 eV is as small as 2.2 meV.

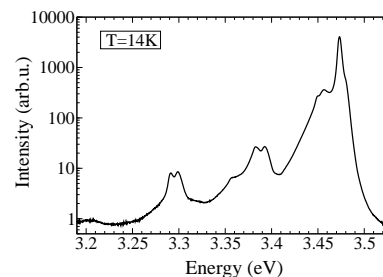


Figure 3 PL spectrum of inverse GaN pyramids recorded at 14 K. The FWHM of the D^0X at 3.479 eV is determined to be as small as 2.2 meV. No stacking fault-related transition observable as typically found in non-polar GaN on foreign substrates [13].

Analyzing the structural properties of the active area of the LED sample using scanning TEM (STEM), well developed GaInN QWs with abrupt interfaces can be observed confirming the high material quality from the optical active region, (Fig. 4).

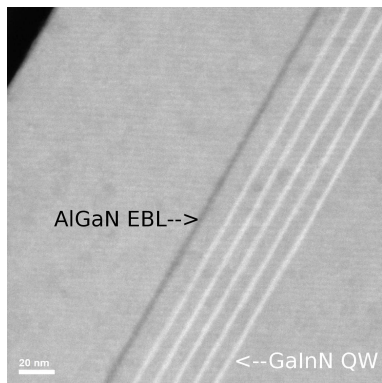


Figure 4 STEM image of semipolar GaInN/GaN LED structure grown on inverse pyramids.

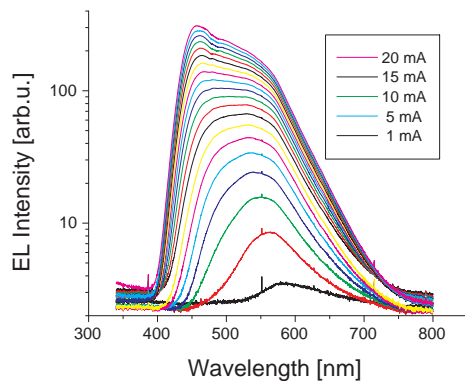


Figure 5 EL spectra of semipolar GaInN/GaN LED grown on inverse GaN pyramids for currents between 1 and 20 mA.

Fig. 5 shows the respective EL spectra recorded for currents between 1 and 20 mA during EL test measurements. A relatively broad emission is detected from the integrally collected light which is not expected when taking into account the reduced piezoelectric field on semipolar surfaces. Whereas for small currents the longer wavelength in the green spectral region is dominating, the emission shifts towards the blue spectral region for higher currents. The exact color coordinate for each current is depicted in Fig. 6. Interestingly, for a current of 1 mA white light can be realized without the use of any phosphor. Furthermore, the coverage of the LED with an orange-red phosphor should open the possibility for the generation of white light with a high color rendering index (CRI) at a high excitation level as there would be no green minimum as often seen in the spectra of commercially available white LEDs.

The unusual shift of the color coordinate within the color diagram can not be simply explained by state filling of potential fluctuations within the QWs when increasing the current. For the 3D surface it is essential to investigate

the local layer properties with respect to the specific position on the sample.

Indeed, a strong influence on the QW emission properties was observed within one single facet when performing spatially resolved SEM-CL investigations [11]. Looking to the wavelength distribution on the 3D surface of an undoped sample with a single GaInN QW grown under similar conditions the following situation can be recognized (Fig. 7): From the c-plane areas no QW emission could be recorded at all. This phenomenon can be understood as the QW thickness on the c-plane areas was determined to be as thick as about 7 nm with a relatively high indium content. Due to the fact of the resulting high piezoelectric field on the c-plane and the unconventionally thick QW, electron and hole wavefunctions get extremely separated. Therefore, the recombination probability is very weak with consequently a completely depressed QW emission. On the other hand, strong luminescence is observed from the semipolar facets. Whereas a longer QW emission wavelength is recorded at the top of the structure it shifts gradually to shorter wavelengths when coming closer to the tip. From the edges where two $\{1\bar{1}01\}$ planes meet each other a shorter and brighter emission can be recorded. Now, one can speculate that the main part of the green emission spectrum during the EL test measurements originates from the upper $\{1\bar{1}01\}$ facets, whereas the blue spectral part has its origin from the edges and the area near the tip, correlated with a possible change of the current distribution over the facet area with increasing applied voltage.

The absolute value of the wavelength shift is very much dependent on the geometry of the sample and the growth conditions chosen for the active area growth. Due to the fact that just a slight change of the QW thickness is determined by analyzing the STEM pictures, the strongest influence on the emission wavelength must result from a difference in the indium composition varying along the facet. Gas phase diffusion and surface migration during the ac-

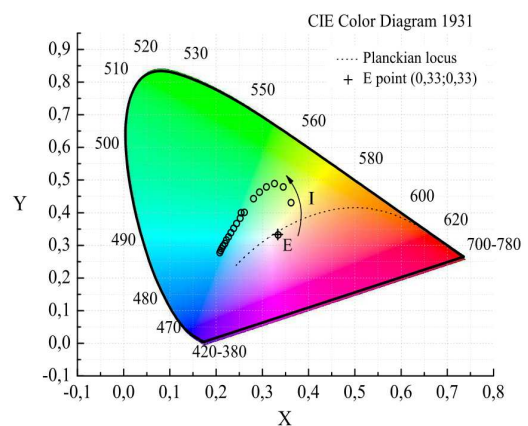


Figure 6 Color coordinates for currents between 1 and 20 mA determined from the respective spectra (see Fig. 5).

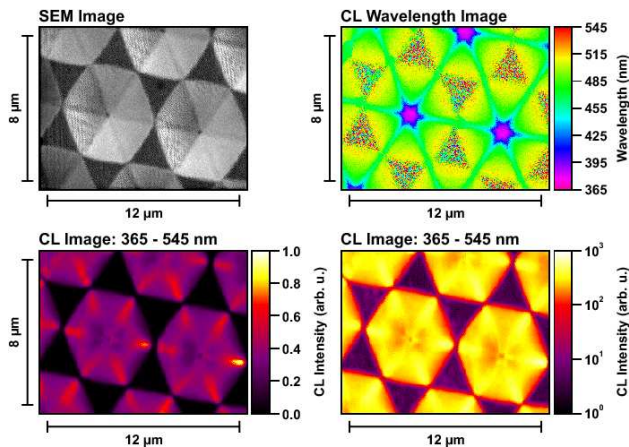


Figure 7 SEM-CL images recorded from an undoped GaInN single QW grown on inverse pyramids with semipolar $\{1\bar{1}0\}$ facets.

tive area growth are drastically reduced due to the growth conditions necessary for a high indium incorporation efficiency. As could be confirmed by ongoing experiments the wavelength shift could be influenced by changing the growth conditions with respect to the diffusion coefficient. E.g. the variation of the reactor pressure during the active area growth influenced the linewidth of the emission [12] and could probably explain the pronounced shift observed by Nishizuka *et al.* for GaInN/GaN stripes with $\{11\bar{2}\}$ facets grown at atmospheric pressure [14].

4 Conclusion Semipolar GaInN/GaN LEDs were realized on the $\{1\bar{1}0\}$ side facets of selectively grown inverse GaN pyramids on full 2 inch sapphire wafers. The excellent material quality was confirmed by TEM and STEM analyses which suggest (nearly) defect free semipolar surfaces. The relatively broad QW emission during electroluminescence test measurements are correlated with the gradually varying QW wavelength emission along one single facet. Its origin is mainly thought to arise from a different indium composition as a result of gas phase diffusion processes during the active area growth as the QW thickness does not change drastically. Furthermore, the dominant peak wavelength is found to be dependent on the applied current density. Those properties could be advantageous for the generation of white light emitters with a high CRI whereas the desired color coordinate can be fine-tuned by the current.

Acknowledgements We gratefully acknowledge the fruitful cooperation with M. Feneberg, I. Tischer, M. Wiedenmann and K. Thonke from the Inst. of Semiconductor Physics, Ulm University. This work was financially supported by the Deutsche Forschungsgemeinschaft (DFG).

References

- [1] P. Waltereit, O. Brandt, A. Trampert, H. Grahn, J. Menniger, M. Ramsteiner, M. Reiche, and K. Ploog, *Nature* **406**, 865 (2000).
- [2] A. Chakraborty, B. Haskell, H. Masui, S. Keller, J. Speck, S. DenBaars, S. Nakamura, and U. Mishra, *Jpn. J. Appl. Phys.* **45**, 739 (2006).
- [3] B. Liu, R. Zhang, Z. L. Xie, C. X. Liu, J. Y. Kong, J. Yao, Q. J. Liu, Z. Zhang, D. Y. Fu, X. Q. Xiu, H. Lu, P. Chen, P. Han, S. L. Gu, Y. Shi, and Y. D. Zheng, *Appl. Phys. Lett.* **91**, 253506 (2007).
- [4] S. Hwang, Y. G. Seo, K. H. Baik, I. Cho, J. H. Baek, S. Jung, T. G. Kim, and M. Cho, *Appl. Phys. Lett.* **95**, 071101 (2009).
- [5] K.-C. Kim, M. Schmidt, H. Sato, F. Wu, N. Fellows, M. Saito, K. Fujito, J. Speck, S. Nakamura, and S. DenBaars, *phys. stat. sol. (RRL)* **1**, 125 (2007).
- [6] U. Schwarz, and M. Kneissel, *phys. stat. sol. (RRL)* **1**, A44 (2007).
- [7] B. Beaumont, P. Vennéguès, and P. Gibart, *phys. stat. sol. (b)* **227**, 1 (2001).
- [8] T. Wunderer, P. Brückner, B. Neubert, F. Scholz, M. Feneberg, F. Lipski, M. Schirra, and K. Thonke, *Appl. Phys. Lett.* **89**, 041121 (2006).
- [9] J. Hertkorn, F. Lipski, P. Brückner, T. Wunderer, S.B. Thapa, F. Scholz, A. Chuvilin, U. Kaiser, M. Beer, and J. Zweck, *J. Cryst. Growth.* **310**, 4867 (2008).
- [10] T. Wunderer, F. Lipski, J. Hertkorn, S. Schwaiger, and F. Scholz, *phys. stat. sol. (c)* **6**, 490 (2009).
- [11] T. Wunderer, F. Lipski, S. Schwaiger, J. Hertkorn, M. Wiedenmann, M. Feneberg, K. Thonke, and F. Scholz, *Jpn. J. Appl. Phys.* **48**, 060201 (2009).
- [12] T. Wunderer, J. Wang, F. Lipski, S. Schwaiger, K. Forghani, and F. Scholz, not published.
- [13] P.P. Paskov, R. Schifano, B. Monemar, T. Paskova, S. Figge, and D. Hommel, *J. Appl. Phys.* **98**, 093519 (2005).
- [14] K. Nishizuka, M. Funato, Y. Kawakami, Y. Narukawa, and T. Mukai, *Appl. Phys. Lett.* **87**, 231901 (2005).